





Seventh Framework Programme FP7-SPACE-2010-1 Stimulating the development of downstream GMES services

Grant agreement for: Collaborative Project. Small- or medium scale focused research project

Project acronym: **SIDARUS**

Project title: Sea Ice Downstream services for Arctic and Antarctic Users

and Stakeholders

Grant agreement no. 262922
Start date of project: 01.01.11
Duration: 36 months

Project coordinator: Nansen Environmental and Remote Sensing Center, Bergen, Norway

D10.31: Promotion material V1

Due date of deliverable: 31.12.2011
Actual submission date: 01.02.2012

Organization name of lead contractor for this deliverable: NERSC

	Project co-funded by the European Commission	_
	within the Seventh Framework Programme, Theme 6 SPACE	
	Dissemination Level	
PU	Public	X
PP	Restricted to other programme participants (including the Commission)	
RE	Restricted to a group specified by the consortium (including the Commission)	
СО	Confidential, only for members of the consortium (including the Commission)	

DATE	CHANGE RECORDS	AUTHOR
01/03/2012	Version 0.1	S. Sandven

SIDARUS CONSORTIUM

Participant no.	Participant organisation name	Short name	Country
1 (Coordinator)	Nansen Environmental and Remote Sensing Center	NERSC	NO
2	Alfred-Wegener-Institut für Polar-und Meeresforschung	AWI	DE
3	Collecte Localisation Satellites SA	CLS	FR
4	University of Bremen, Institute of Environmental Physics	UB	DE
5	The Chancellor, Masters and Scholars of the University of Cambridge	UCAM	UK
6	Norwegian Meteorological Institute, Norwegian Ice Service	Met.no	NO
7	Scientific foundation Nansen International Environmental and Remote Sensing Centre	NIERSC	RU
8	B.I. Stepanov Institute of Physics of the National Academy of Sciences of Belarus	IPNASB	BR

No part of this work may be reproduced or used in any form or by any means (graphic, electronic, or mechanical including photocopying, recording, taping, or information storage and retrieval systems) without the written permission of the copyright owner(s) in accordance with the terms of the SIDARUS Consortium Agreement (EC Grant Agreement 262922).

All rights reserved.

This document may change without notice

Table of Contents

1	HIGH-RESOLUTION ICE INFORMATION FROM SAR IMAGES	2
2	SEA ICE CONCENTRATION COMBINED WITH ANIMAL TRACKING	6
3	SEA ICE THICKNESS DATA FOR CLIMATE RESEARCH	8
	SEA ICE ALBEDO	
5.	ICE FORECASTING IN THE BARENTS SEA	12

SUMMARY

This report presents the first set of promotion material, consisting of a set of figures and text showing products and services that SIDARUS is developing. These figures are used in contacts with users and are presented at the public web site of SIDARUS. The promotion material will be updated towards the end of the project.

1 High-resolution ice information from SAR images

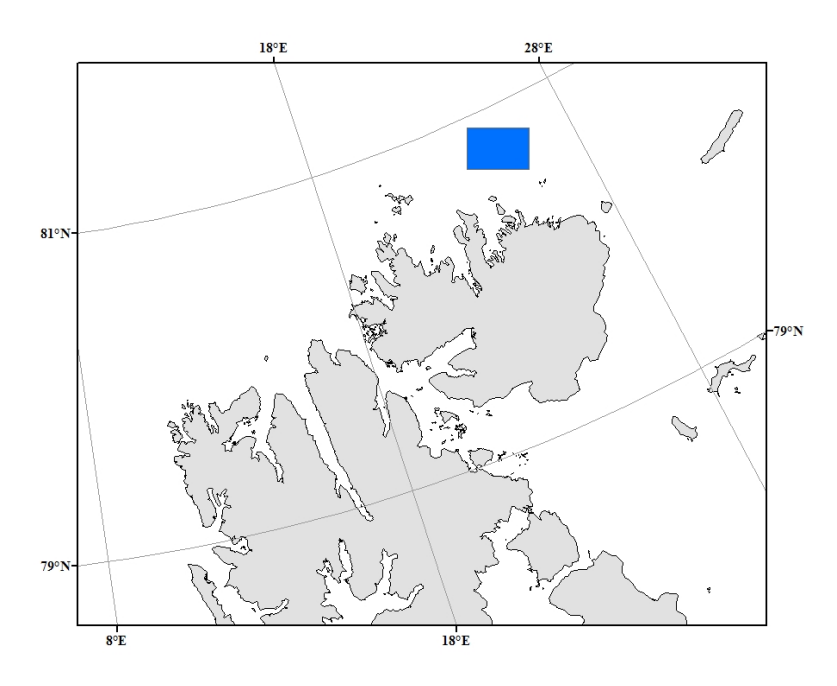


Figure 1, a map of north of Svalbard showing the coverage area for the following satellites images examples.

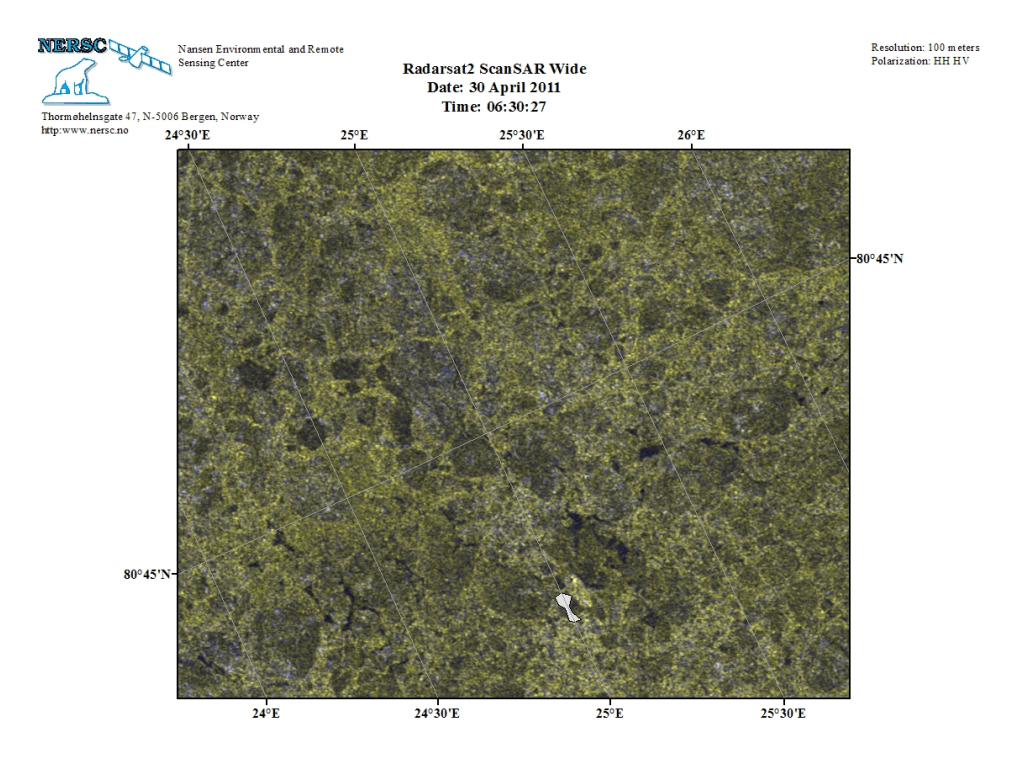


Figure 2, Radarsat-2 SAR images with dual polarization, where the HH channel is projected in red and green and the HV channel is project in blue to produce an RGBimage..

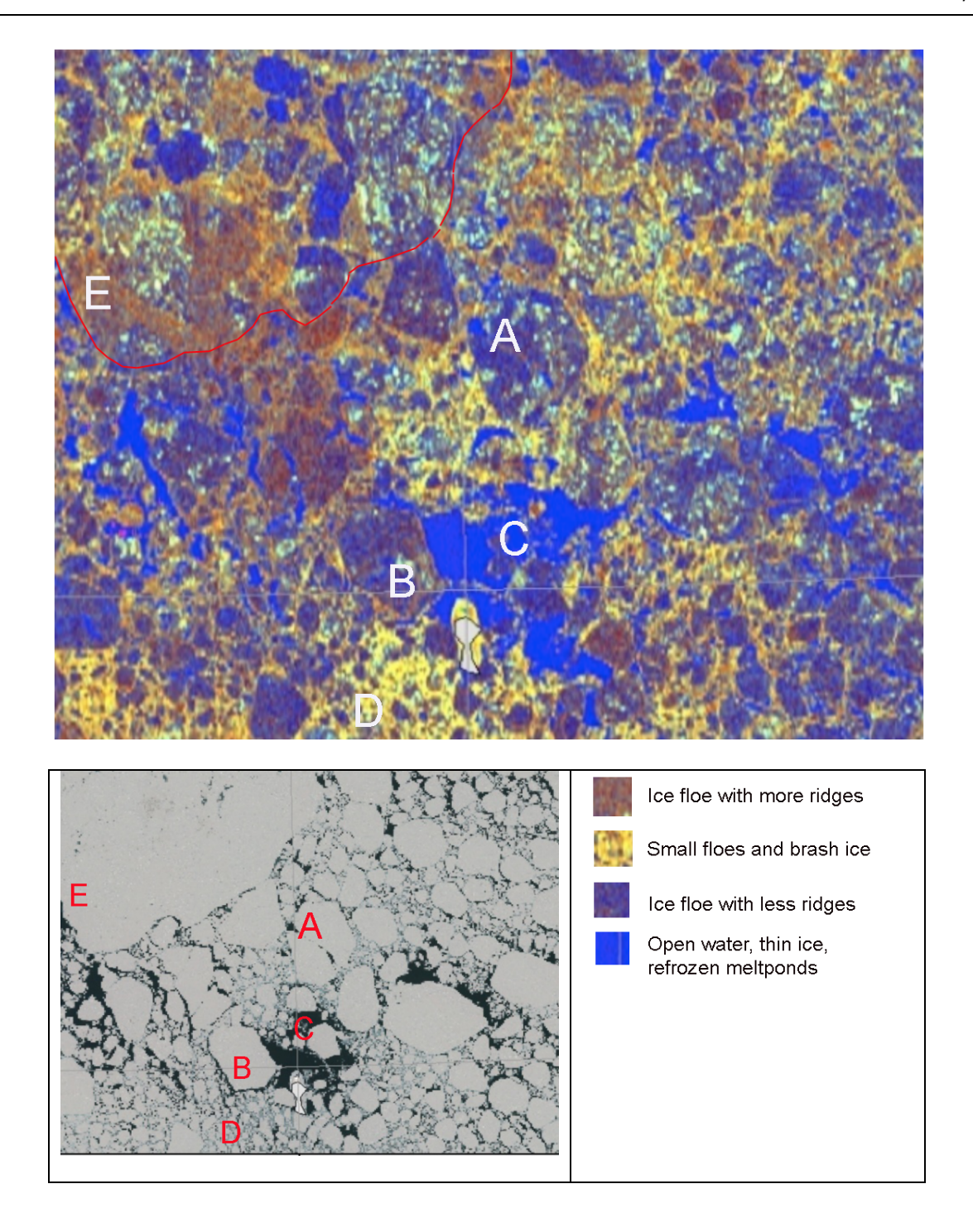


Figure 3.Upper image: classification of a Radarsat2 Fine Quad-Pol images dated 30 April 2011, located as shown in Fig. 1. The classification uses HH and the HV channels in combination and the results is presented in colour code identifying four typical ice characeristics, as shown in the legend below. The image is high resolution (10 m prixel size) showing more details compared to ScaSAR Wideswath HH/HV image in Fig. 2. The lower left figure show and subset of an optical SPOT image, covering the same area as the Radarsat-2 classified image. High-resolution optical images are only available during cloudfree conditions, but will be useful for validating the results of the SAR classification.

06 February /2008

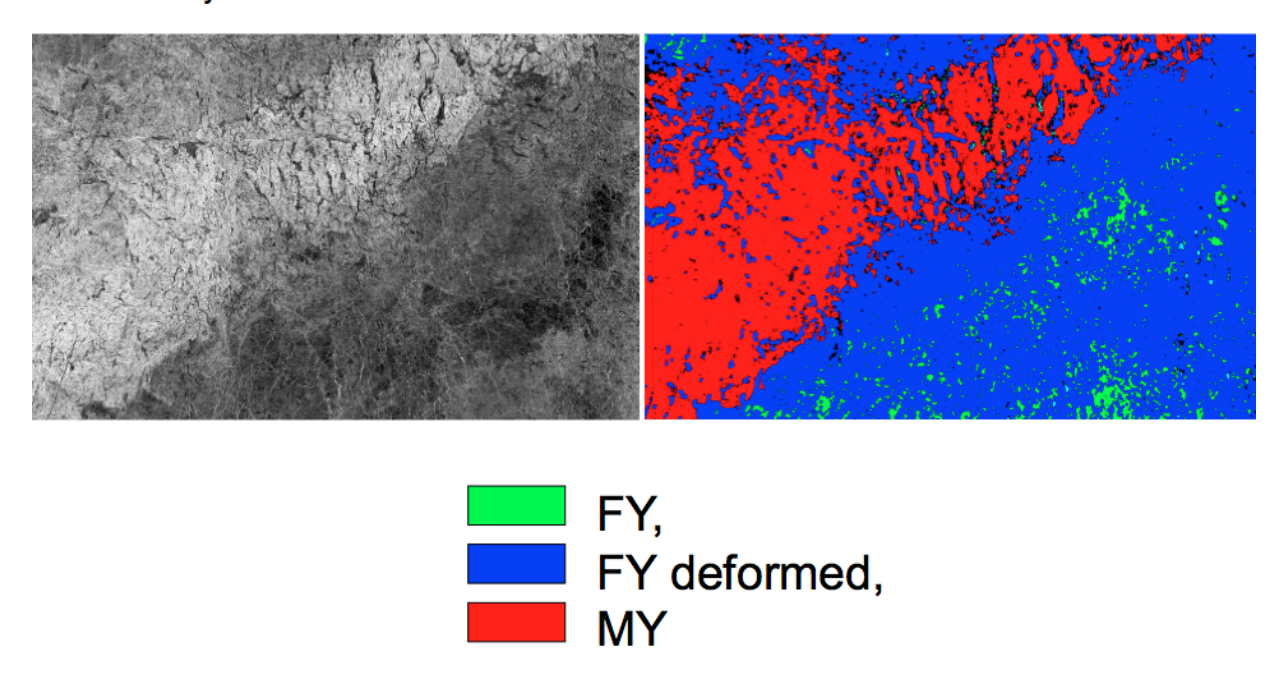


Figure 4. Classification of multiyear and firstyear icea (level and deformed) in an ENVISAT ASAR images of 06 February 2008 using the neural network algorithm developed by Zakhvatkina et al, (2012).

07 February 2008

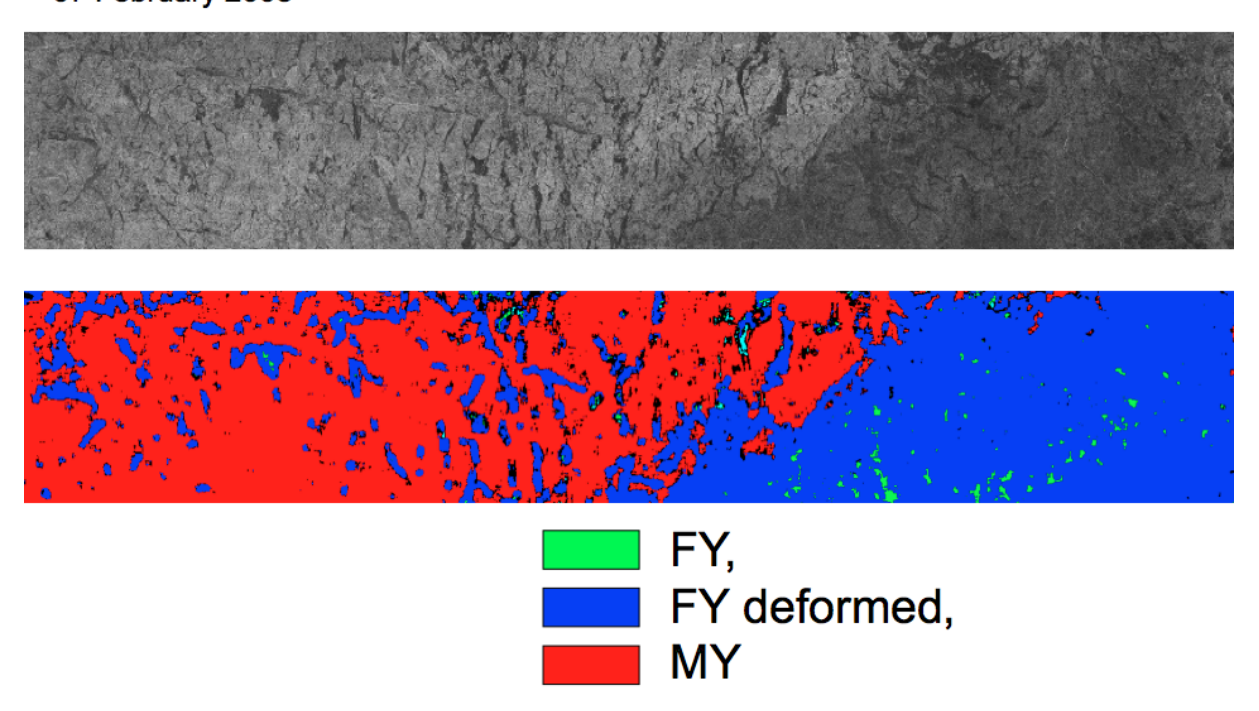


Figure 5. Classification of multiyear and firstyear icea (level and deformed) in an ENVISAT ASAR image of 07 February 2008 using the neural network algorithm developed by Zakhvatkina et al, (2012).

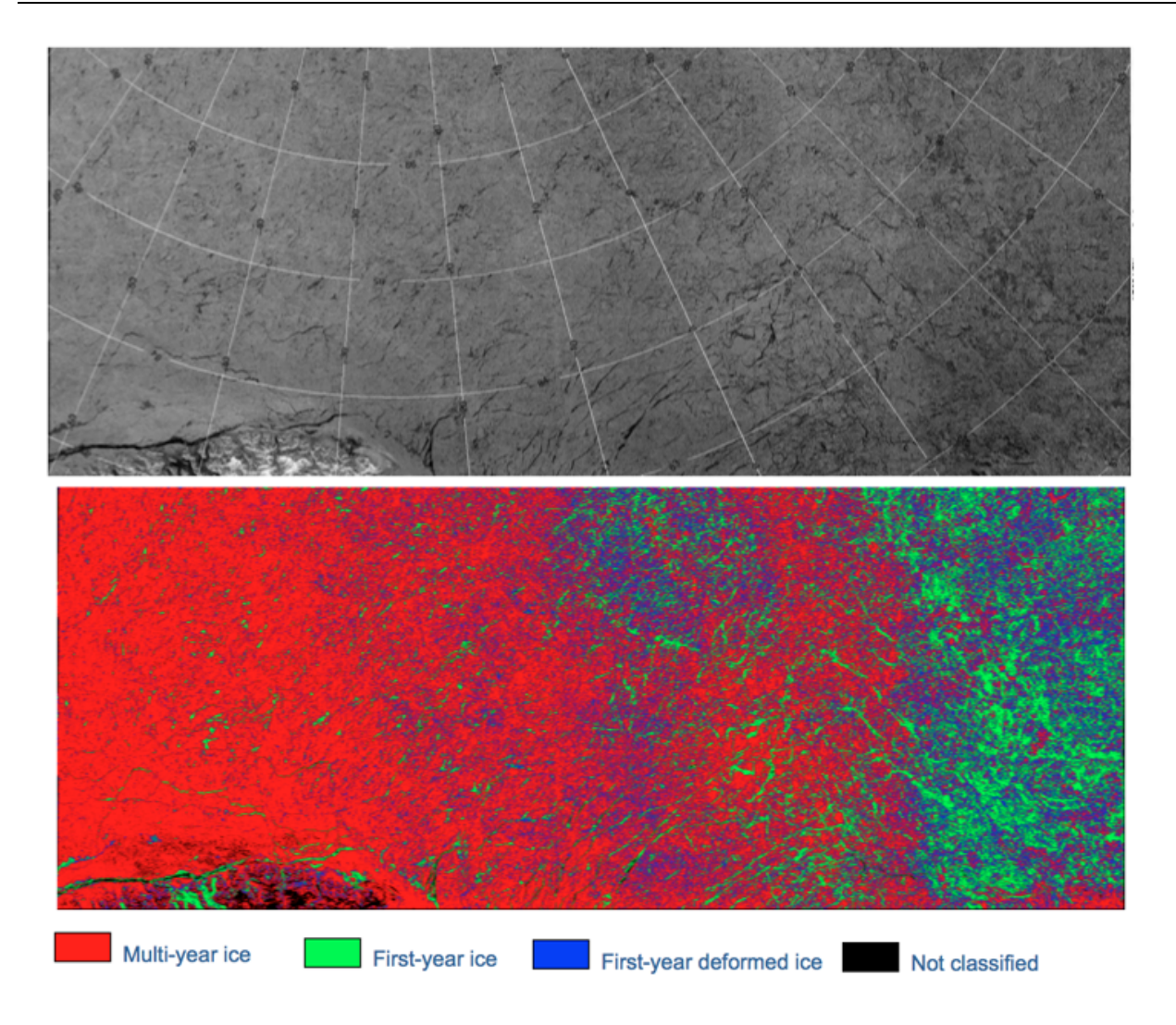


Figure 6. Classification of multiyear and firstyear icea (level and deformed) in an ENVISAT ASAR image of 11 January 2011 using bayesian algorithm developed by Zakhvatkina et al, (2012)

2 Sea ice concentration combined with animal tracking

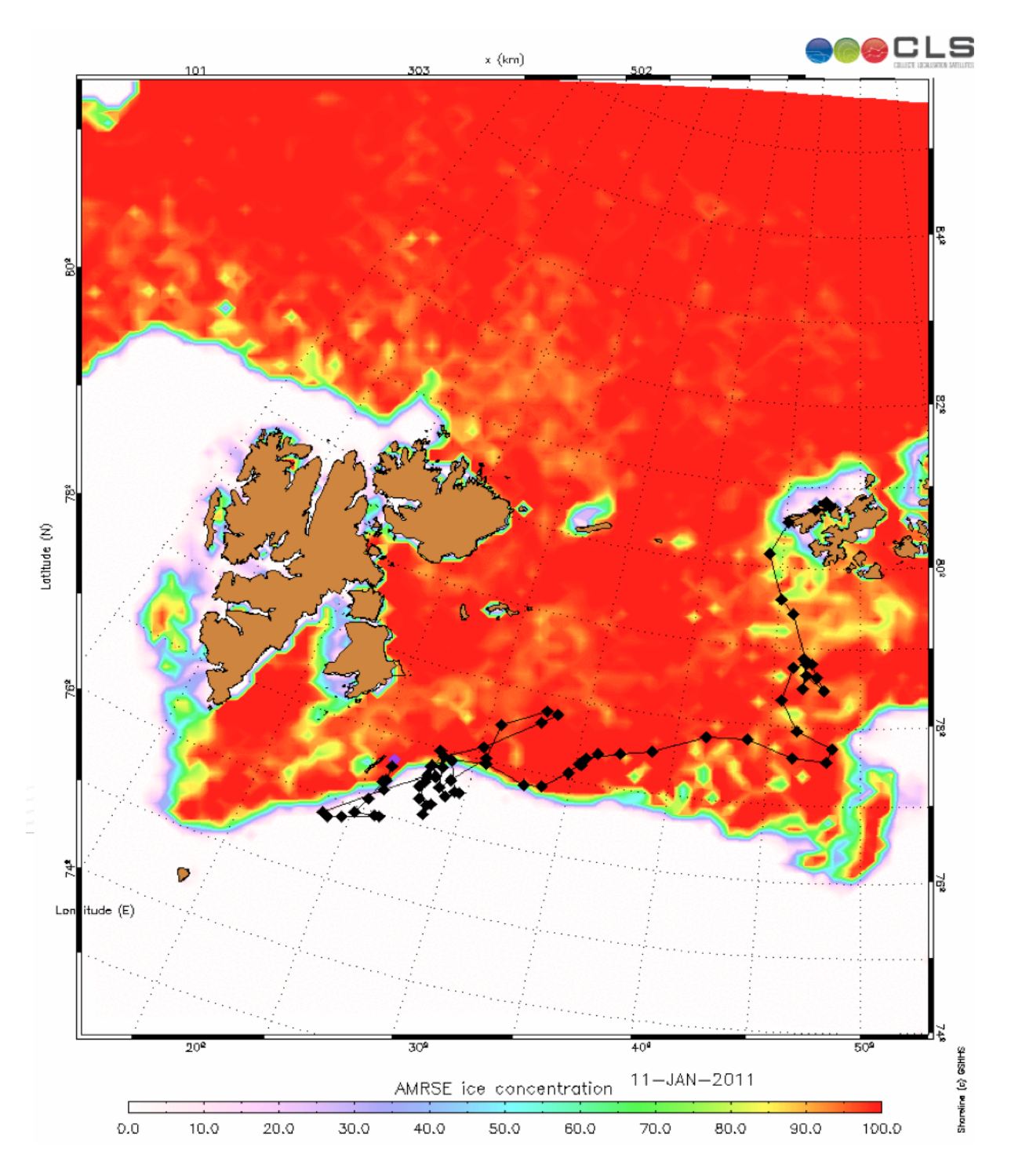


Figure 7. Polarbear track from September 2010 to April 2011 for bear with Argos ID 103383. The track starts on northern Franz Josef Land and ends near Hopen island. The ice concentration map is from 11 January 2011, based on AMSRE data.

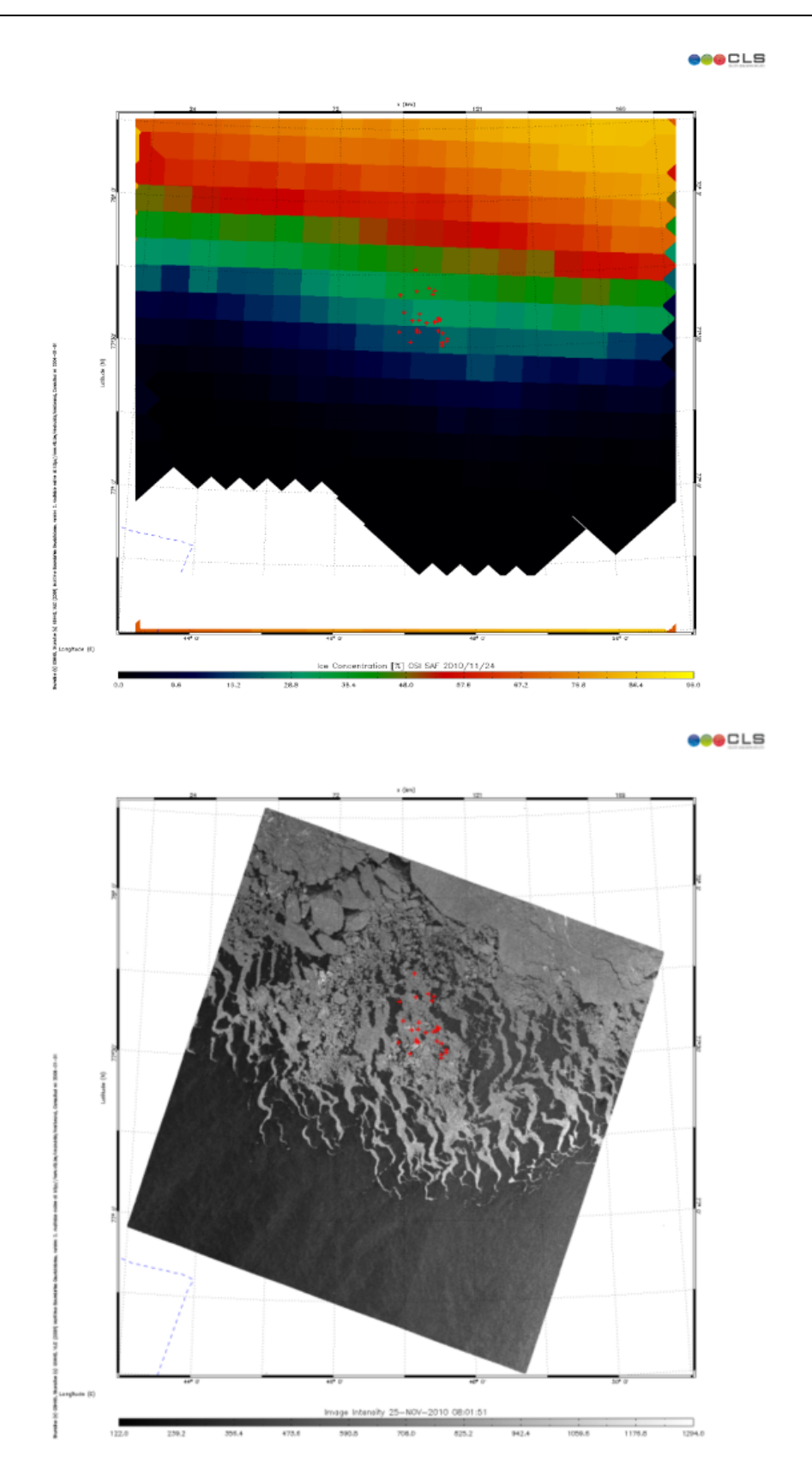


Figure 8. Upper image: Ice concentration map from OSI SAF from 24 November 2010 with polarbear positions superimposed by red dots in an area where ice concentration is 30 - 50 % (green pixels). Lower mage: SAR image from 25 November 2010 with the same polarbear positions. The data is from the Barents Sea south of Franz Josef Land (44° - 50° E).

3 Sea ice thickness data for climate research

UK submarines have conducted cruises in the Arctic where ice draft has been measured by sonars since 1971. These data, combined with data from US submarines, represent a major data source for studies of ice thickness variability and trends over the last decades.



Figure 9. Picture of HMS Dreadnought

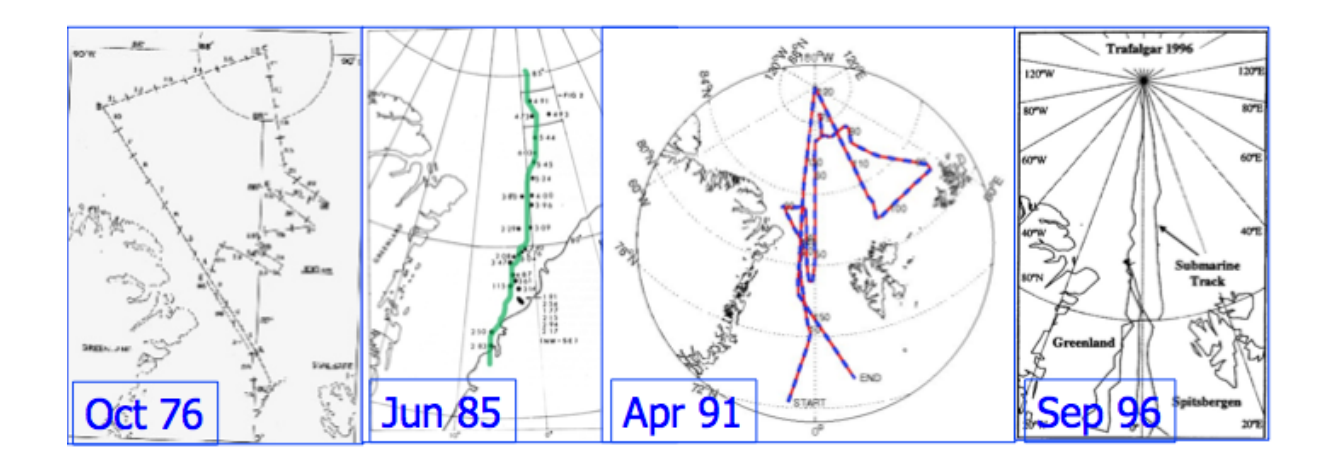


Figure 10. Tracks of UK submarine cruises where ice draft data were collected.

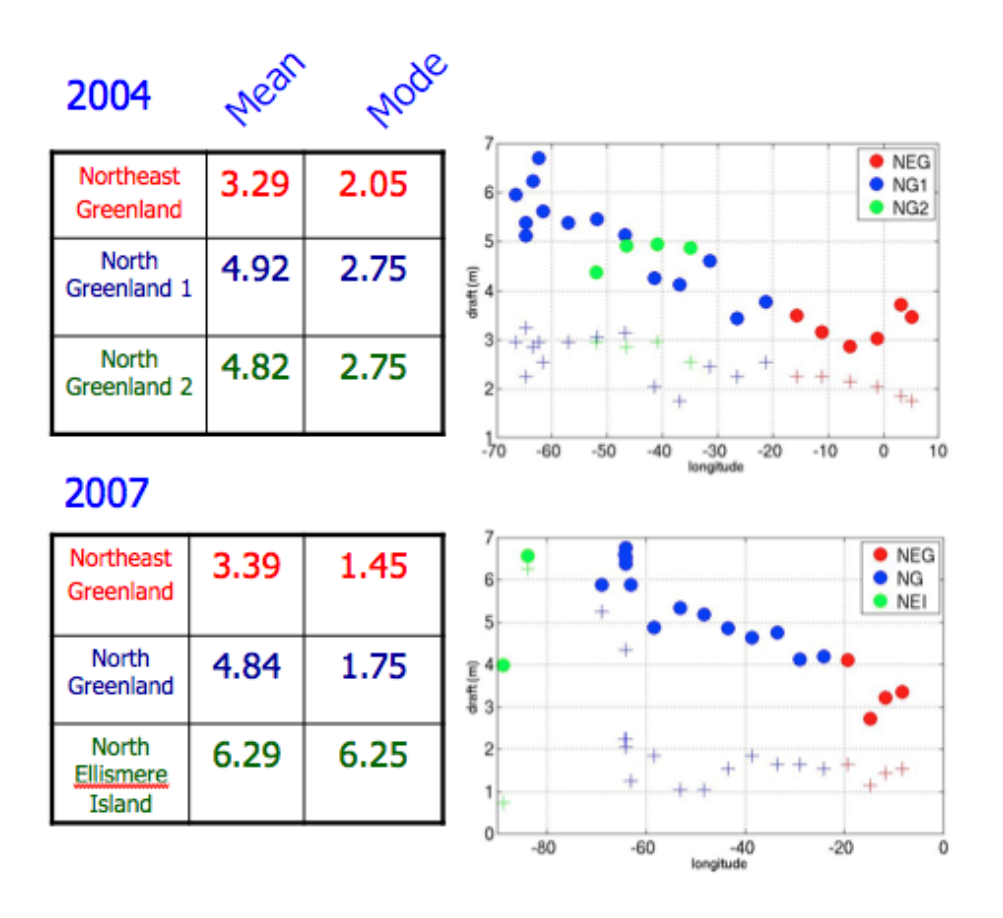


Figure 11. Mean and modal draft of the ice north of Greenland in 2004 and 2007.

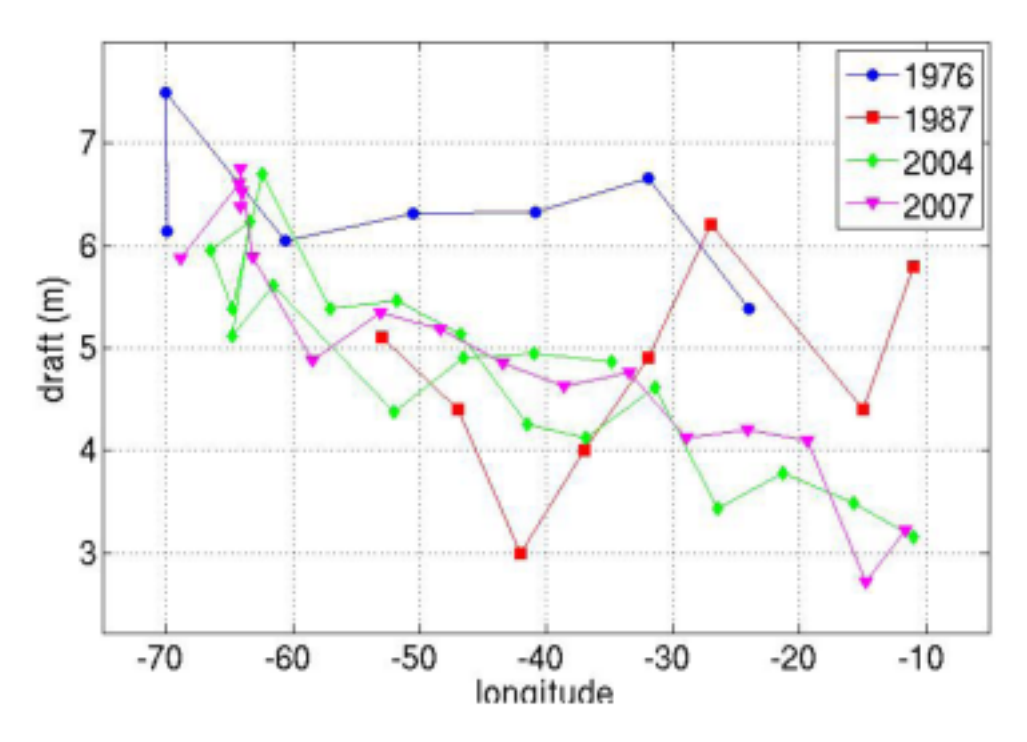


Figure 12. Mean draft north of Greenland and in the Fram Strait in east-west section at approximately 85°N from cruises in 1976, 1987, 2004 and 2007.

Ice thickness is also measured by airborne electromagnetic induction device operated from a helicopter or a fixed-wing aircraft (Fig 14). AWI has conducted such surveys for many years in the Arctic.Rhe results show how the thickness distribution has changed in the last two decades. The panels in Fig. 13 show thickness variability in different parts of the Arctic sea ice areas.

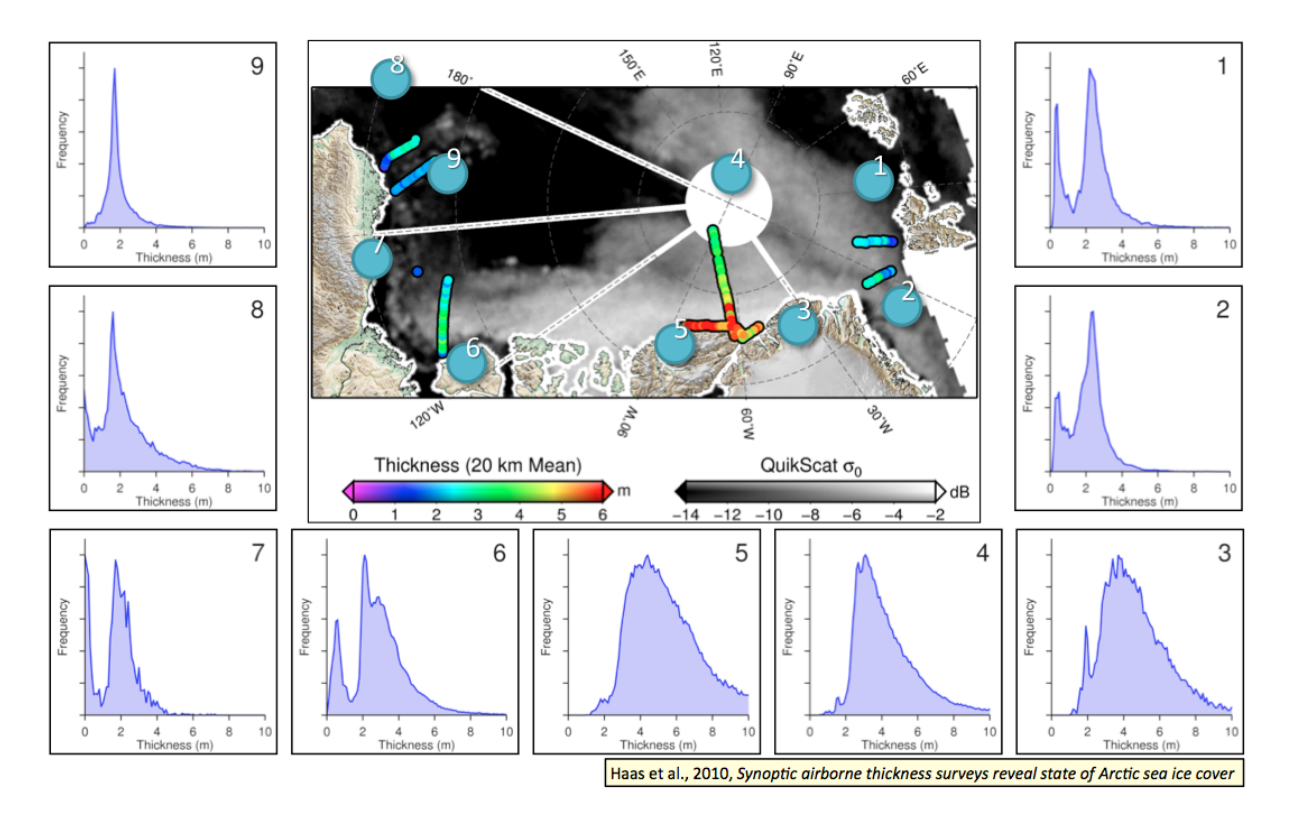


Figure 13. Ice thickness distributions in different parts of the Arctic (Haas et al., 2010).

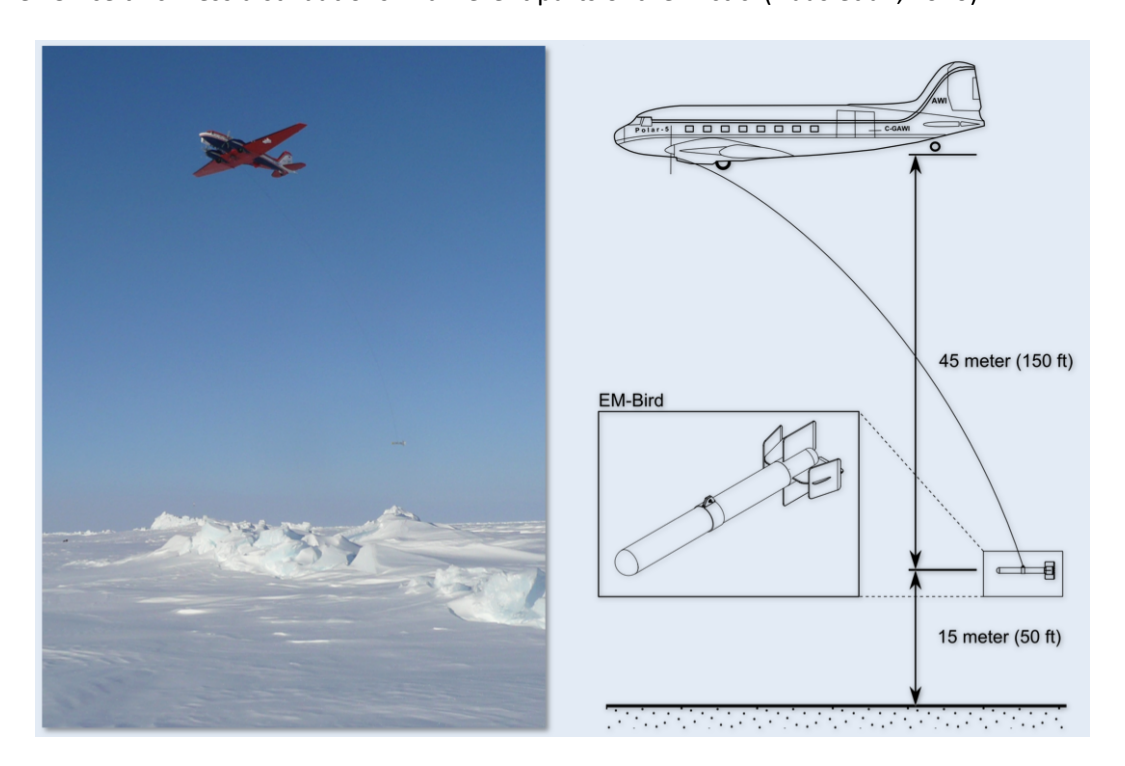


Figure 14. POLAR-5 aircraft flying EM bird (Left) and illustration of the observing system (AWI, 2010)

4 Sea ice albedo

The high albedo of snow and sea ice covered areas plays a crucial role for the energy balance of the Arctic. The temperature – albedo feedback mechanism can enhance the global warming in the Polar regions through th efollowing steps: rising temperature increases melting of snow and ice, which reduces the surfce albedo, which in turn increases the solar absorbtion and enhances the warming. Correct modeling of the albedo is therefore important for general circulation models (GCMs) and numerical weather and sea ice prediction models.

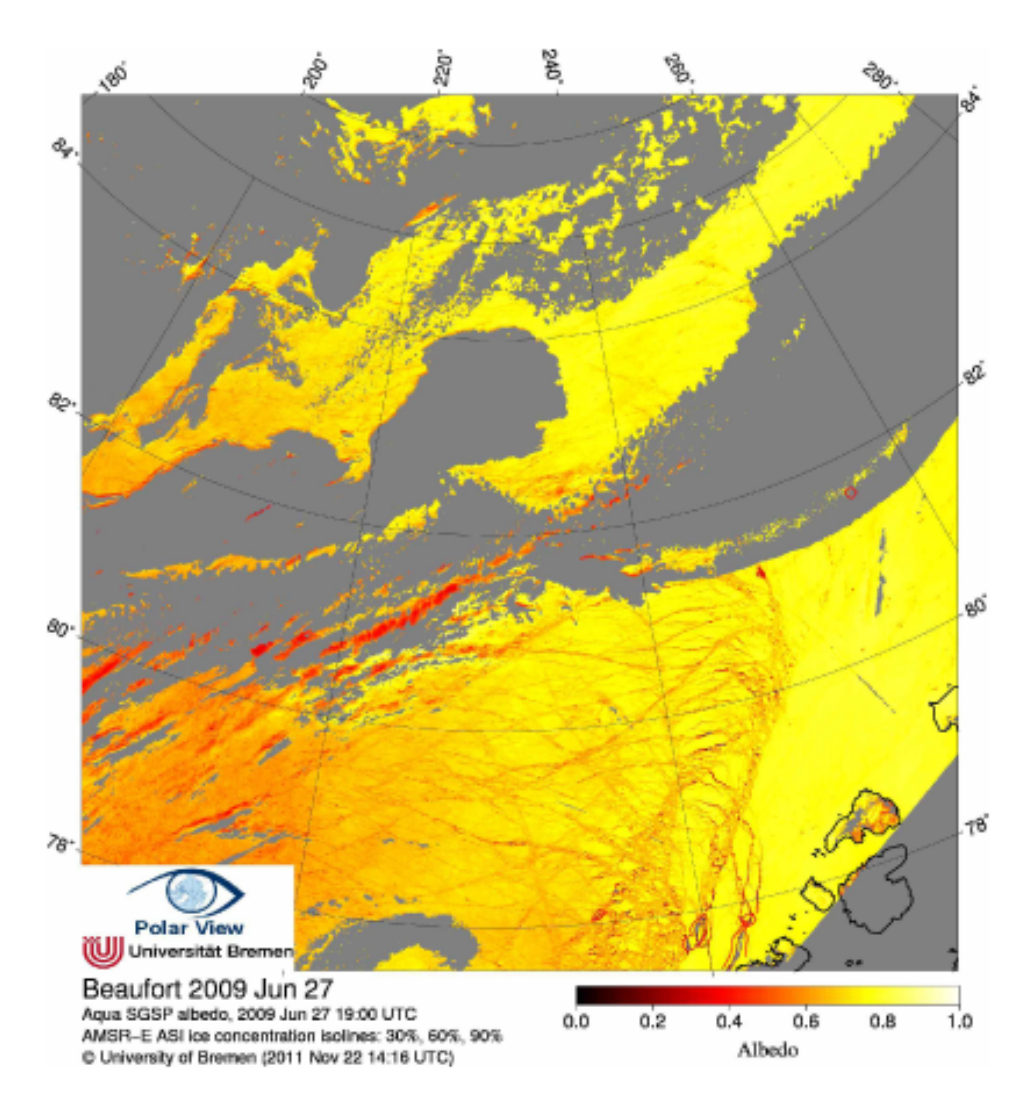


Figure 15. Example of ice albedo retrieved from averaging of MODIS reflectance of three visible bands (1, 2, and 3). The grey areas are cloud-masked.

5. Ice forecasting in the Barents Sea

The TOPAZ ice-ocean forcasting system in MyOcean provides lateral boundary conditions to a nested 4 km resolution HYCOM model of the Barents Sea, that includes tides and resolves better the mesoscale activity in the Barents Sea (Fig 16 a). In order to provide more accurate sea ice forecasting in the Barents Sea, a regional high-resolution model will be used operationally in order to provide ice forecasts to offshore operators in the region.

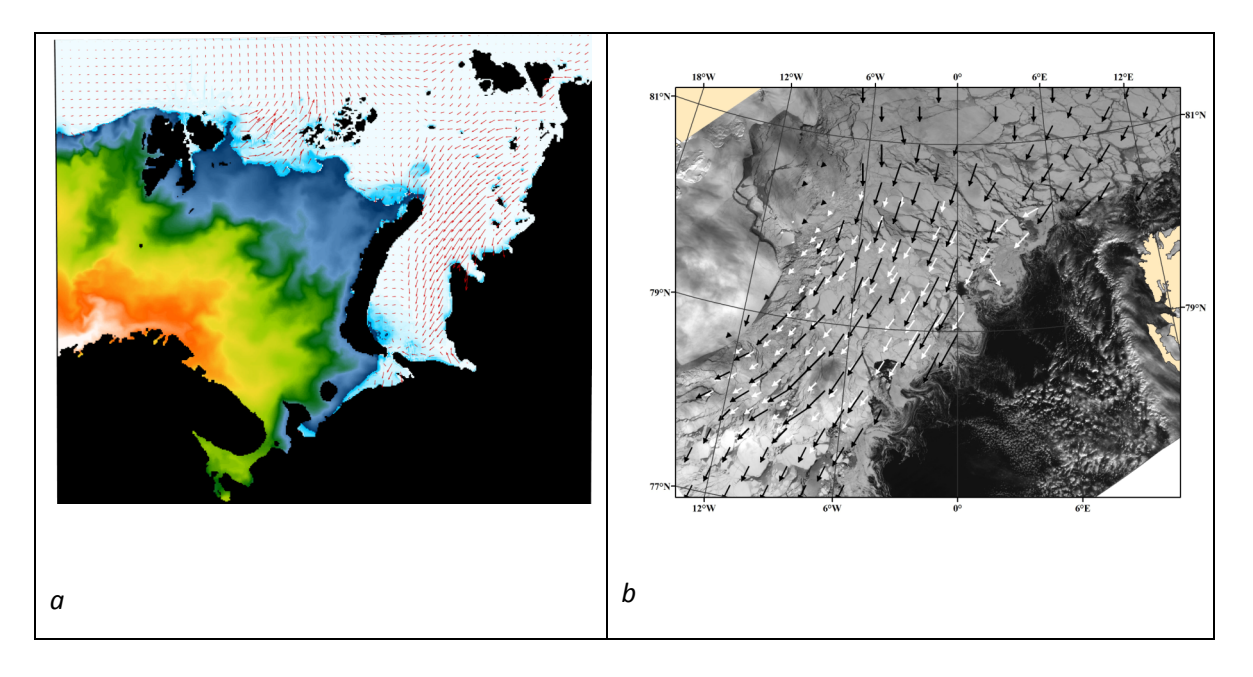


Figure 16 (a) Example of modeled ice-ocean in the Barents Sea region using the 4 km HYCOM model forced at the boundary by the TOPAZ system, where colour code indicates SST and arrows show ice drift. (b) ice drift data from satellite observations: white arrows are from SAR analysis, black arrows are from MODIS analysis.

END OF DOCUMENT